Phys Chem Minerals (2017) 44:75–82
DOI 10.1007/s00269-016-0838-1

ORIGINAL PAPER

Spryite, $Ag_8\left(As^{3+}_{0.5}As^{5+}_{0.5}\right)S_6$: structure determination and inferred absence of superionic conduction of the first As^{3+}-bearing argyrodite

Luca Bindi[1] · Frank N. Keutsch[2] · Marta Morana[3] · Federica Zaccarini[4]

Received: 10 May 2016 / Accepted: 10 August 2016 / Published online: 20 August 2016

Abstract We report data on the composition and crystal structure of the first As^{3+}-bearing natural argyrodite, spryite. Spryite has the formula $(Ag_{7.98}Cu_{0.05})_{\Sigma=8.03}(As^{5+}_{0.31}Ge_{0.36}As^{3+}_{0.31}Fe^{3+}_{0.02})_{\Sigma=1.00}S_{5.97}$, ideally $Ag_8(As^{3+}_{0.5}As^{5+}_{0.5})S_6$. The crystal studied was found in a sample from the Uchucchacua polymetallic deposit, Oyon district, Cajatambo, Lima Department, Peru. The structure was refined in the space group $Pna2_1$ up to $R = 0.0782$ using 2099 observed reflections [$2\sigma(I)$ level]. Spryite is intimately twinned with six twin domains. The structure solution showed that As^{3+} and As^{5+} coexist in the new mineral, which represents the first case ever discovered in either a mineral or a synthetic compound belonging to a sulfide/sulfosalt group. High-temperature in situ X-ray diffraction experiments indicated that no phase transitions occur in the temperature range investigated and that the mineral does not show any evidence of fast ionic conduction.

✉ Luca Bindi
luca.bindi@unifi.it

[1] Dipartimento di Scienze della Terra, Università degli Studi di Firenze, Via La Pira 4, 50121 Florence, Italy

[2] Department of Chemistry and Chemical Biology, John A. Paulson School of Engineering and Applied Sciences, Harvard University, Cambridge, MA 02138, USA

[3] Dipartimento di Chimica "Ugo Schiff", Università degli Studi di Firenze, Via della Lastruccia 3, Sesto Fiorentino, 50019 Florence, Italy

[4] Department of Applied Geosciences and Geophysics, University of Leoben, Peter Tunner Str. 5, 8700 Leoben, Austria

Keywords Argyrodite · Fast ionic conductors · Crystal structure · Ag-sulfosalts

Introduction

About 130 years ago, in the summer of 1885, an Ag-rich opaque mineral of unusual appearance was found at *Himmelsfürst Fundgrube* near Freiberg, Germany. Weisbach (1886) recognized it as a new mineral species and called it argyrodite. Such a discovery in nature was a breakthrough because, the same year, the German chemist Winkler demonstrated that it contained a new element: germanium (Winkler 1886), which represented clear evidence for Dmitri Mendeleev's concept of periodicity and the periodic table. Nowadays, argyrodite-type compounds are very numerous and deeply studied for their manifold structural and physical properties. They exhibit the general formula $A^{m+}_{[(12-n-y)/m]}B^{n+}Q^{2-}_{6-y}X^{-}_{y}$, with mono- or divalent twofold or threefold coordinated A cations (Cu^{+}, Ag^{+}, Li^{+}, Cd^{2+}, Hg^{2+}), tri-, tetra-, or pentavalent tetrahedral B cations (Al^{3+}, Ga^{3+}, Si^{4+}, Ge^{4+}, Sn^{4+}, Ti^{4+}, P^{5+}, As^{5+}, Sb^{5+}, Nb^{5+}, Ta^{5+}), and chalcogenide Q (O^{2-}, S^{2-}, Se^{2-}, Te^{2-}) and/or halide X (Cl^{-}, Br^{-}, I^{-}) ions as anions (Kuhs et al. 1979). These compounds are known to be fast ionic conductors or semiconductors and as such find practical applications in silver photography as sensitizers, in optics and microelectronics as rewritable storage media, and as electrolytes (Evain et al. 1998; Gaudin et al. 2001; Rao and Adams 2011; Frank et al. 2013; Chen et al. 2015). In order to understand their physical properties, an exact knowledge of the crystal structure of the compound is indispensable. These compounds undergo three phase transitions as a function of temperature: The high-temperature phase crystallizes in the space group $F\,\bar{4}\,3\,m$; the medium-temperature phase,

usually refined using a non-harmonic technique [Gram–Charlier expansion of the atomic displacement factors (Zucker and Schulz 1982; Bindi and Evain 2007)], has the space group $P2_13$; and the low-temperature phase has apparent space group $F\,\overline{4}\,3\,m$, but actually adopts an orthorhombic symmetry (space groups $Pna2_1$, $Pnam$, or $Pmn2_1$).

Here we report a heretofore unobserved compound belonging to the argyrodite group exhibiting the ideal formula $Ag_8(As^{3+}_{0.5}As^{5+}_{0.5})S_6$. It represents the first As^{3+}-bearing member of the argyrodite group. It occurs in nature and was found in the Ag- and Mn-rich zone of the Uchucchacua polymetallic deposit, Oyon district, Cajatambo, Lima Department, Peru, a complex vein-type deposit related to a dacitic intrusion cutting through Cretaceous and Tertiary formations on the West side of the Occidental Cordillera of Central Andes (Oudin et al. 1982).

The mineral, approved by the IMA-NMNC Commission (2015-116) and named spryite after Paul G. Spry (b. 1955), professor of economic geology at the Iowa State University (USA), crystallizes with orthorhombic symmetry, space group $Pna2_1$, and the type specimen is deposited in the Mineralogical Collection of the Museo di Storia Naturale, Università degli Studi di Firenze, Via La Pira 4, Florence, Italy, catalogue number 3213/I. Among the tetrahedrally coordinated B atoms in the argyrodite structure, only three trivalent cations have been reported, i.e., Al^{3+}, Ga^{3+}, and Fe^{3+} in the mineral chenguodaite (Gu et al. 2003, 2008; Frank et al. 2013). Trivalent As was never thought to enter the argyrodite structure because of the stereochemical activity of the lone-pair electrons, which makes the tetrahedral coordination impossible for As^{3+}. Motivated by the recovery of such As^{3+}-bearing mineral with the argyrodite structure, we carried out a single-crystal X-ray diffraction investigation at room temperature to study the structural changes occurring when the $½As^{3+} + ½As^{5+} \rightarrow Ge^{4+}$ substitution takes place. Furthermore, given the fact that most Ag^+–Cu^+-containing argyrodites exhibit strong structural disorder due to the high mobility of the monovalent cations linked to their strong ionic conductivity (e.g., Gaudin et al. 2001), we also performed in situ single-crystal X-ray diffraction experiments in the temperature range 90–500 K to see the effects of As^{3+} on the general thermal behavior of the mineral.

Materials and methods

Sample

The sample containing spryite originates from a specimen obtained by one of the authors (F.N.K.) from the mineral dealer Jorge Luis Rojas Leandro as part of a study of a silver and manganese-rich zone of the Uchucchacua polymetallic deposit, Oyon district, Cajatambo, Lima Department, Peru. Spryite is associated with proustite, argyrodite, and microscopic galena in a Mn-bearing calcite matrix (Fig. 1).

Fig. 1 Spryite, $Ag_8(As^{3+}_{0.5}As^{5+}_{0.5})S_6$, equant crystals surrounding proustite (Ag_3AsS_3) crystals on Mn–calcite. Field of view 1.6 cm

Physical and optical properties

Spryite is metallic and black in color. It has a black streak, non-fluorescent, with a Mohs hardness of 2½–3; VHN_{20} range is 55–70, with a mean of 67 kg mm^{-2}. It is brittle, with no cleavage. Density was not measured because of the small amount of available material. The calculated density on the basis of the empirical formula and X-ray single-crystal data is 6.334 g cm^{-3}. In plane-polarized incident light, spryite is weakly to moderately bireflectant and weakly pleochroic from dark gray to a dark green. Internal reflections are absent. Between crossed polars, the mineral is weakly anisotropic, without characteristic rotation tints. The reflectance was measured in air by means of a MPM-200 Zeiss microphotometer equipped with a MSP-20 system processor on a Zeiss Axioplan ore microscope. Filament temperature was approximately 3350 K. Readings were taken for specimen and standard (SiC) maintained under the same focus conditions. The diameter of the circular measuring area was 0.1 mm. Reflectance values (R_{min} and R_{max}) at wavelengths approximating the four COM-recommended wavelengths are: 26.4, 26.9 (471.1 nm), 24.7, 25.0 (548.3 nm), 24.4, 24.8 (586.6 nm), 24.5, 24.8 (652.3 nm).

Chemical analysis

A preliminary chemical analysis using EDS performed on the crystal fragment used for the structural study did not indicate the presence of elements ($Z > 9$) other than Fe, Cu, As, Ag, Ge, and S. Analyses (seven spot analyses) were

Table 1 Analytical data (mean and ranges in wt%) and standard deviations (SD) for spryite

Constituent	Mean	Ranges	SD
Ag	76.12	74.34–78.71	0.90
Cu	0.30	0.20–0.39	0.05
Fe	0.09	0.05–0.16	0.03
Ge	2.31	1.69–2.64	0.11
As	4.07	3.41–4.43	0.12
S	16.93	15.74–17.66	0.28
Total	99.82	99.01–101.37	0.50

carried out using a Superprobe Jeol JXA 8200 microprobe (WDS mode, 20 kV, 10 nA, 1 μm beam size). For WDS analyses, the following lines were used: Ag*L*α, Cu*K*α, Fe*K*α, Ge*L*α, As*L*α, S*K*α. The standards were: Ag metal (Ag), chalcopyrite (Cu, Fe), Ge metal (Ge), skutterudite (As), and galena (S). The crystal fragment was found to be homogeneous within analytical error. Analytical data are given in Table 1. The empirical formula (based on 15 atoms per formula unit and on the structural results—see below) is $(Ag_{7.98}Cu_{0.05})_{\Sigma=8.03}(As^{5+}_{0.31}Ge_{0.36}As^{3+}_{0.31}Fe^{3+}_{0.02})_{\Sigma=1.00}S_{5.97}$, ideally $Ag_8(As^{3+}_{0.5}As^{5+}_{0.5})S_6$.

Table 2 Crystal and experimental data for spryite

Crystal data	
Crystal size (mm)	0.030 × 0.040 × 0.070
Cell setting, space group	Orthorhombic, $Pna2_1$
a, *b*, *c* (Å)	14.984(4), 7.474(1), 10.571(2)
V (Å^3)	1083.9(4)
Z	4
Data collection and refinement	
Radiation, wavelength (Å)	Mo*K*α, λ = 0.71073
Temperature (K)	293
$2\theta_{max}$	60.30
Measured reflections	13,910
Unique reflections	2317
Reflections with $I > 2\sigma(I)$	2099
R_{int}	0.054
*R*σ	0.038
Range of *h*, *k*, *l*	$-21 \le h \le 21$, $-10 \le k \le 10$, $-14 \le l \le 14$
R [$F_o > 4\sigma(F_o)$]	0.0782
R (all data)	0.0816
wR (on F^2)	0.1190
GooF	1.126
Twin matrices	$T1\begin{bmatrix}1&0&0\\0&1&0\\0&0&1\end{bmatrix}T2\begin{bmatrix}1/2&1/4&1/2\\-1&-1/2&1\\1&-1/2&0\end{bmatrix}$
	$T3\begin{bmatrix}1/2&-1/4&1/2\\1&-1/2&-1\\1&1/2&0\end{bmatrix}T4\begin{bmatrix}0&-1/2&0\\2&0&0\\0&0&-1\end{bmatrix}$
	$T5\begin{bmatrix}-1/2&1/4&-1/2\\1&-1/2&-1\\1&1/2&0\end{bmatrix}T6\begin{bmatrix}1/2&1/4&-1/2\\1&1/2&1\\-1&1/2&0\end{bmatrix}$
Twin volume fractions	0.26(5), 0.21(3), 0.19(3), 0.13(3), 0.11 (3), 0.10(3)
Number of least-squares parameters	43
Max. and min. resid. peak (*e* Å^{-3})	2.04–2.03

Table 3 Atom coordinates, site-occupancy factors (s.o.f.), and equivalent isotropic displacement parameters (Å^2) for spryite

Site	s.o.f.	*x/a*	*y/b*	*z/c*	U_{eq}
Ag1	$Ag_{1.00}$	0.1270(3)	0.2229(5)	0.3768(4)	0.050(1)
Ag2	$Ag_{1.00}$	0.0620(3)	0.2261(5)	0.8375(4)	0.051(1)
Ag3	$Ag_{1.00}$	0.4325(3)	0.0615(5)	0.0195(4)	0.050(1)
Ag4	$Ag_{1.00}$	0.2766(3)	0.5000(5)	0.0824(5)	0.051(1)
Ag5	$Ag_{1.00}$	0.4185(3)	0.0907(5)	0.6964(5)	0.051(1)
Ag6	$Ag_{1.00}$	0.2727(3)	0.3843(5)	0.6840(5)	0.051(1)
Ag7	$Ag_{1.00}$	0.0171(3)	0.0110(5)	0.6027(4)	0.050(1)
Ag8	$Ag_{1.00}$	0.2587(3)	0.1283(5)	0.9055(4)	0.050(1)
*M*1	$(Ge_{0.38}As^{5+}_{0.30})_{\Sigma=0.68(1)}$	0.3758(6)	0.229(1)	0.350(1)	0.051(2)
*M*2	$As^{3+}_{0.32(1)}$	0.376(1)	0.068(2)	0.268(2)	0.051(2)
S1	$S_{1.00}$	0.122(1)	0.489(2)	0.977(2)	0.052(3)
S2	$S_{1.00}$	−0.004(1)	0.271(2)	0.231(2)	0.054(3)
S3	$S_{1.00}$	0.373(1)	0.467(2)	0.479(1)	0.049(3)
S4	$S_{1.00}$	0.258(1)	0.232(2)	0.230(2)	0.057(3)
S5	$S_{1.00}$	0.386(1)	0.315(2)	0.865(2)	0.064(4)
S6	$S_{1.00}$	0.1230(9)	0.267(2)	0.612(1)	0.044(3)

Single-crystal X-ray diffraction at room temperature

The same crystal used for the electron microprobe analysis was used for the single-crystal X-ray diffraction study which was done with an Oxford Diffraction Xcalibur 3 diffractometer (X-ray Mo*K*α radiation, $\lambda = 0.71073$ Å) fitted with a Sapphire 2 CCD detector (see Table 2 for details). In expectation of possible crystal twinning, a full diffraction sphere was collected. The diffraction pattern was apparently consistent with cubic symmetry ($a \approx 10.5$ Å). Intensity integration and standard Lorentz–polarization corrections were done with the *CrysAlis* RED (Oxford Diffraction 2006) software package. The program ABSPACK of the *CrysAlis* RED package (Oxford Diffraction 2006) was used for the absorption correction. Subsequent calculations were conducted with the JANA2006 program suite (Petříček et al. 2006).

LT and HT-single-crystal X-ray diffraction

By means of a Helijet cooling/heating device (Oxford Diffraction 2006) mounted on the same single-crystal diffractometer, the same crystal was then studied in the temperature range 90–500 K. We started from low temperature and raised the temperature with a heating rate of 15 K/h. The temperature fluctuations were less than ±1.5 K throughout the temperature range. Unit-cell parameters are given in Table 4. Before each measurement, the sample was held at the specified temperature for 60 min. As a check, after the measurement at 500 K, the crystal was re-cooled at 350 and 300 K. The unit-cell values obtained did not reveal significant variations from those previously measured, indicating that no hysteresis occurs within the temperature range examined.

Results

Structure determination

From the analysis of the set of intensities, the highest symmetry point group appeared to be $\bar{4}\ 3\ m$ ($R_{int} = 0.11$). However, the structures of pure argyrodite, Ag_8GeS_6, and canfieldite, Ag_8SnS_6, are reported as orthorhombic [$a = 15.15$, $b = 7.48$, $c = 10.59$ Å, $V = 1200.1$ Å^3 and $a = 15.30$, $b = 7.55$, $c = 10.70$ Å, $V = 1236.0$ Å^3, for argyrodite (Eulenberger 1977) and canfieldite (Wang 1978; Bindi et al. 2012), respectively]. The relationships between the orthorhombic and cubic unit cells are easy to describe: (1) The cubic unit cell with $a \approx 10.5$ Å corresponds to the orthorhombic *c* axis of argyrodite; (2) the diagonal of the face of the cube with $a \approx 10.5$ Å is very close to the real orthorhombic *a* axis of argyrodite; and (3) the diagonal of the face of the cube with $a \approx 10.5$ Å divided by 2 is very close to the real orthorhombic *b* axis of argyrodite. From this geometric consideration, it was then obvious that the cubic symmetry was not correct and the reflection data set was transformed in the orthorhombic cell (i.e., $a \approx 15$, $b \approx 7.5$ Å, and $c \approx 10.5$ Å) and averaged accordingly in the orthorhombic symmetry ($R_{int} = 0.054$), taking into account the twin law that makes the twin lattice cubic. To generate the $\bar{4}\ 3\ m$ point group from the *mm*2 subgroup, six twin laws are required (Table 2): *E*, 3[111], 3^2[111], $\bar{4}$ [001], $\bar{4}$ [010], and *m*[011] (herein labeled *T*1, *T*2, *T*3, *T*4, *T*5, and *T*6, respectively). Taking into account the twin laws, all reflections could be indexed with the new cell and agreed with the $Pna2_1$ space group. The structure refinement was initiated in the $Pna2_1$ space group, starting from the atomic coordinates reported for synthetic Ag_8GeS_6 (Eulenberger 1977). Given the large number of atoms in the starting structural model, the site-occupancy refinement of most of the metal positions, and the use of anisotropic atomic displacement parameters for all the atoms, a severe damping factor (<0.1) was used in the full-matrix refinement. After several cycles, an ordered solution with full site occupations was finally determined by carefully removing atoms with low site occupations and/or non-realistic distances with neighboring atoms and adding significant positions found in the difference Fourier syntheses. The refinement of the occupancy factors for all Ag (Ag vs. structural vacancy) and S (S vs. structural vacancy) atoms produced site-scattering values consistent with pure Ag and S, respectively. On the other hand, the position usually occupied by Ge in argyrodite (Eulenberger 1977), here labeled *M*1, was found to be partially occupied (Table 3), and a new position (*M*2) at about 1.5 Å from *M*1 was found. The new

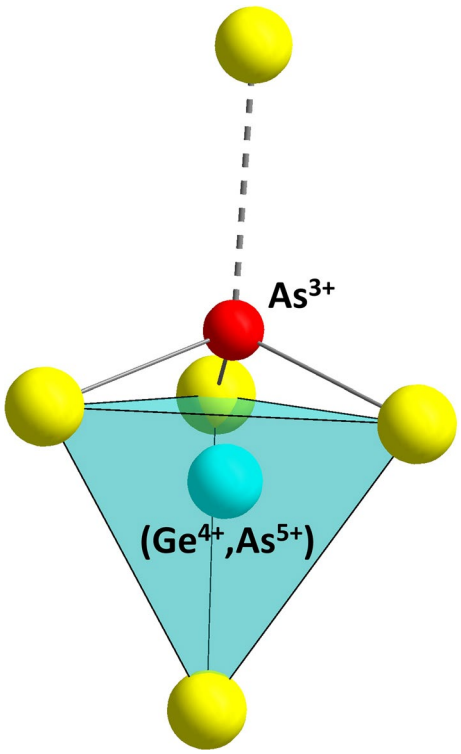

Fig. 2 Portion of the crystal structure of spryite highlighting the split *M*1–*M*2 positions (see text for explanation). In *light blue* the *M*1 tetrahedron and with a *red circle* the *M*2 atom

*M*2 position exhibited a complementary occupancy with *M*1. We thus refined the occupancy of *M*1 versus *M*2 by fixing the same atomic displacement parameters for the two atoms. Noteworthy, the atoms in *M*1 exhibit a perfect tetrahedral environment whereas those in *M*2 a trigonal pyramidal coordination (see Fig. 2). Furthermore, the mean electron number refined at the *M*1 site was 22.4, well matching the population $As^{5+}_{0.31}Ge_{0.36}Fe^{3+}_{0.02}$ (mean electron number 22.3). Likewise, the mean electron number at the *M*2 site (10.6) is

Table 5 Selected bond distances (Å) for spryite

Ag1–S6	2.50(1)	Ag6–S6	2.53(1)
Ag1–S4	2.51(2)	Ag6–S5	2.61(2)
Ag1–S2	2.52(2)	Ag6–S4	2.69(1)
⟨Ag1–S⟩	2.51	Ag6–S3	2.71(2)
		⟨Ag6–S⟩	2.64
Ag2–S6	2.58(1)		
Ag2–S1	2.61(1)	Ag7–S6	2.48(1)
Ag2–S3	2.63(1)	Ag7–S2	2.52(1)
Ag2–S5	2.67(2)	Ag7–S3	2.53(1)
⟨Ag2–S⟩	2.62	⟨Ag7–S⟩	2.51
Ag3–S6	2.55(1)	Ag8–S5	2.40(2)
Ag3–S5	2.59(2)	Ag8–S3	2.44(2)
Ag3–S2	2.74(2)	⟨Ag8–S⟩	2.42
Ag3–S1	2.91(2)		
⟨Ag3–S⟩	2.70	*M*1–S4	2.17(2)
		*M*1–S3	2.24(2)
Ag4–S6	2.52(1)	*M*1–S2	2.19(2)
Ag4–S4	2.55(2)	*M*1–S1	2.25(2)
Ag4–S1	2.57(2)	⟨*M*1–S⟩	2.21
⟨Ag4–S⟩	2.55		
		*M*2–S4	2.19(2)
Ag5–S5	2.49(2)	*M*2–S2	2.19(2)
Ag5–S1	2.52(2)	*M*2–S1	2.28(3)
Ag5–S2	2.74(1)	⟨*M*2–S⟩	2.22
⟨Ag5–S⟩	2.58		

Table 4 Anisotropic displacement parameters for spryite

	U^{11}	U^{22}	U^{33}	U^{12}	U^{13}	U^{23}
Ag1	0.049(3)	0.051(2)	0.051(3)	−0.0004(19)	0.000(2)	−0.0026(19)
Ag2	0.049(3)	0.051(2)	0.054(3)	0.0012(19)	−0.002(2)	0.0009(19)
Ag3	0.048(3)	0.051(2)	0.052(2)	−0.001(2)	0.002(2)	−0.0045(19)
Ag4	0.049(3)	0.050(2)	0.054(3)	0.0004(19)	0.001(2)	−0.0046(19)
Ag5	0.048(3)	0.051(2)	0.054(3)	0.0003(19)	0.001(2)	−0.0006(19)
Ag6	0.049(3)	0.052(2)	0.052(2)	−0.0005(19)	−0.003(2)	−0.0020(19)
Ag7	0.049(3)	0.050(2)	0.050(2)	−0.0002(19)	0.000(2)	0.0007(17)
Ag8	0.050(3)	0.053(2)	0.047(2)	−0.0012(18)	0.000(2)	0.004(2)
*M*1	0.050(6)	0.051(4)	0.053(5)	0.000(4)	−0.004(5)	0.001(4)
*M*2	0.050(6)	0.051(4)	0.053(5)	0.000(4)	−0.004(5)	0.001(4)
S1	0.050(10)	0.048(7)	0.058(9)	0.001(6)	−0.002(7)	−0.003(7)
S2	0.049(9)	0.052(7)	0.059(9)	−0.004(6)	0.005(8)	0.004(6)
S3	0.045(9)	0.049(6)	0.053(8)	0.001(6)	0.001(7)	−0.002(6)
S4	0.049(9)	0.054(8)	0.069(11)	0.004(7)	−0.008(9)	−0.006(7)
S5	0.042(8)	0.051(7)	0.100(16)	0.000(6)	0.008(10)	−0.010(9)
S6	0.051(9)	0.047(7)	0.035(7)	−0.002(5)	0.003(6)	−0.006(5)

Table 6 Unit-cell parameters of spryite in the temperature range 90–500 K

T(K)	*a* (Å)	*b* (Å)	*c* (Å)	*V* (Å^3)
90	14.888(2)	7.421(1)	10.408(2)	1149.9(3)
120	14.908(2)	7.429(1)	10.419(2)	1153.9(3)
150	14.919(2)	7.435(1)	10.428(2)	1156.7(3)
175	14.930(2)	7.441(1)	10.435(2)	1159.3(3)
200	14.939(3)	7.448(1)	10.441(2)	1161.7(3)
225	14.950(3)	7.454(1)	10.447(2)	1164.2(3)
250	14.962(3)	7.461(1)	10.452(2)	1166.8(3)
275	14.974(3)	7.469(2)	10.460(2)	1169.9(3)
300	14.985(3)	7.475(2)	10.469(2)	1172.7(3)
325	14.996(3)	7.481(2)	10.480(2)	1175.7(3)
350	15.011(4)	7.488(2)	10.488(2)	1178.9(4)
375	15.023(4)	7.496(2)	10.497(2)	1182.1(4)
400	15.036(4)	7.504(2)	10.505(2)	1185.3(4)
425	15.045(4)	7.511(2)	10.514(3)	1188.1(4)
450	15.057(4)	7.516(2)	10.522(3)	1190.8(4)
475	15.068(5)	7.522(3)	10.533(3)	1193.8(5)
500	15.080(5)	7.529(3)	10.540(3)	1196.7(5)

very close to that calculated considering the As^{3+} content obtained from the electron microprobe analyses (i.e., 10.2).

It became evident that As is present in both the 3+ and 5+ valence states in spryite. Given the crystal-chemical preference for the different cations occurring in spryite, As^{5+} was thought mixed with Ge^{4+} at the *M*1 position, with As^{3+} in the split *M*2 position. Taking into account the refined occupancies for *M*1 and *M*2 sites (68 and 32 %, respectively), the fact that As and Ge show a very close scattering power and the electron microprobe analyses on the crystal used for the structural study, the following structural formula was obtained: $Ag_8[(Ge_{0.36}As^{5+}_{0.32})^{M1}_{\Sigma=0.68}(As^{3+})^{M2}_{\Sigma=0.32}]S_6$. At the last stage, with anisotropic atomic displacement parameters for all atoms and no constraints, the residual value settled at $R = 0.0782$ for 2099 independent observed reflections [$2\sigma(I)$ level] and 141 parameters and at $R = 0.0816$ for all 2317 independent reflections. Further details of the refinement, atom coordinates and isotropic displacement parameters are given in Tables 2 and 3. Anisotropic displacement parameters are reported in Table 4. Bond distances are given in Table 5.

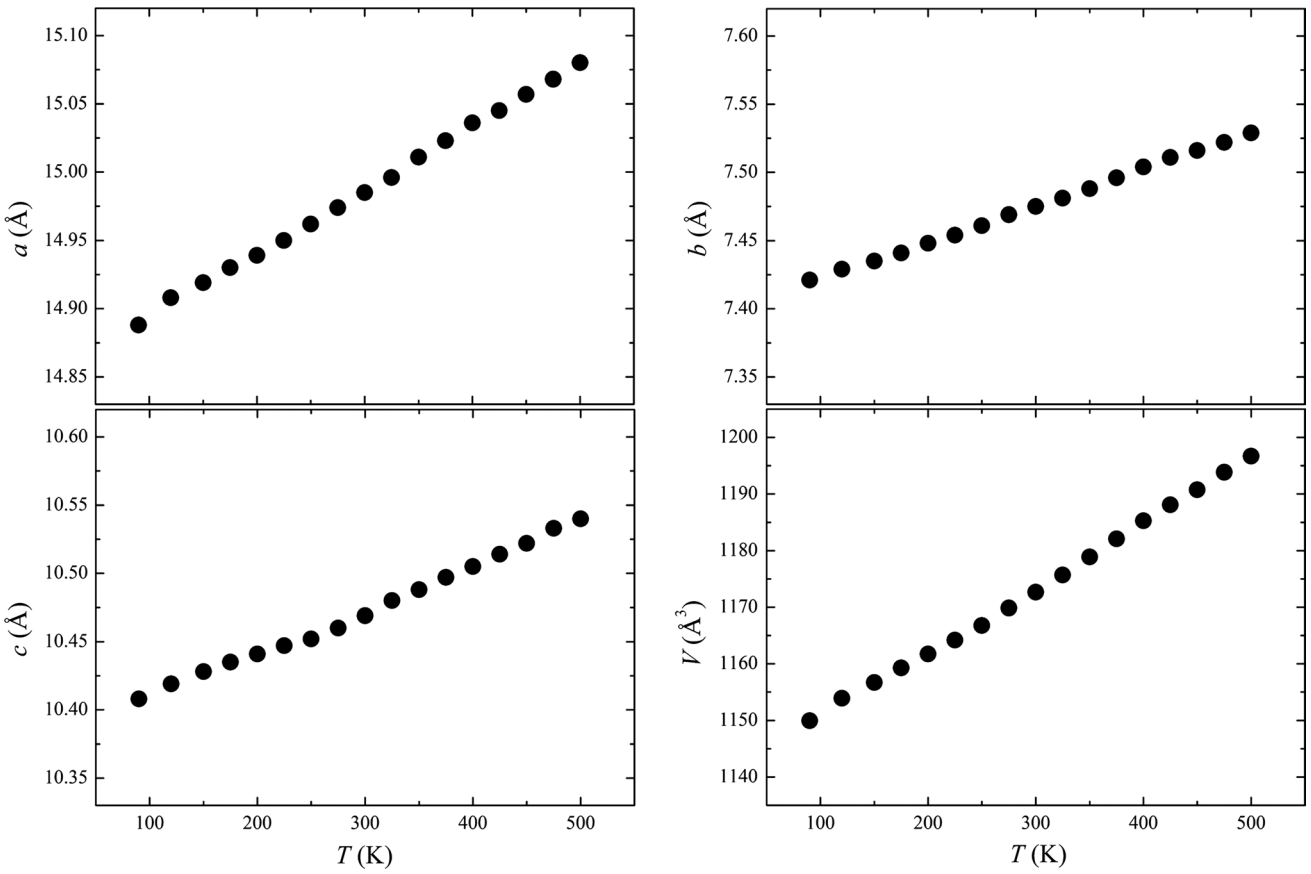

Fig. 3 Variation of the lattice parameters of spryite as a function of temperature

High- and low-temperature behavior

To study the thermal behavior, the same spryite crystal was studied by in situ high-temperature X-ray single-crystal diffraction. From the variation of the unit-cell parameters (Table 6; Fig. 3), it appears evident that no phase transformations occur in the temperature range investigated and that only normal thermal expansion affects the lattice parameters. Spryite maintains an orthorhombic structure over the temperature range (90–500 K), and it represents the first argyrodite-type compound which does not show phase transitions and does not behave as a fast ionic conductor.

Calculated X-ray powder pattern

Table 7 reports the X-ray powder pattern for spryite. Intensities and d_{hkl} values were calculated using PowderCell 2.3 software (Kraus and Nolze 1996) on the basis of the structural model given in Table 3; only reflections with $I_{calc} > 5$ are listed. The strongest reflections are given in bold.

Table 7 Calculated X-ray powder diffraction data (d in Å) for spryite

I_{calc}	d_{calc}	$h\ k\ l$	I_{calc}	d_{calc}	$h\ k\ l$
14	6.1125	201	9	2.4256	223
23	6.1027	011	13	2.4249	031
14	3.7395	212	11	2.3938	131
8	3.6259	120	11	2.3643	214
29	**3.1925**	**411**	22	2.3641	230
9	3.1886	203	18	2.3113	611
7	3.1872	013	11	2.2285	132
24	3.1175	113	7	2.1833	513
31	**3.0563**	**402**	12	2.1814	331
100	**3.0514**	**022**	5	2.1577	024
13	2.9922	320	6	2.1381	522
23	2.9900	122	14	2.0375	603
6	2.9329	213	25	2.0374	621
9	2.8289	412	12	2.0347	205
6	2.8260	222	7	2.0342	035
29	**2.7815**	**510**	6	1.9633	215
11	2.6900	511	10	1.9481	523
68	**2.6868**	**313**	7	1.8851	531
12	2.6456	420	**37**	**1.8697**	**424**
8	2.6428	004	8	1.7906	811
29	**2.6039**	**322**	5	1.7877	415
12	2.5666	403	6	1.7037	116
10	2.5665	421	5	1.6120	035
12	2.5270	123	10	1.5942	442
18	2.4973	600	7	1.5772	633
8	2.4922	204	6	1.5533	912
33	**2.4615**	**512**	8	1.5257	044
26	2.4578	114	8	1.5182	326
17	2.4275	413	6	1.3779	833

Discussion

Spryite is intimately twinned with six twin domains. Arsenic is present in both trivalent and pentavalent state. As^{3+} forms AsS_3 pyramids typical of sulfosalts, (Ge^{4+}, As^{5+}) links four sulfur atoms in a tetrahedral coordination, and Ag occupies sites with coordination ranging from quasi linear to almost tetrahedral connected into a framework (Fig. 4; Table 5). It appears evident that the $M1$ tetrahedron (containing As^{5+} and Ge^{4+} with very similar ionic radii, 0.39 and 0.335 Å, respectively; Shannon 1976) is comparable (mean bond distance 2.21 Å) to pure $Ge^{4+}S_4$ tetrahedra [(2.212 Å in argyrodite (Eulenberger 1977) and 2.192 Å in putzite (Paar et al. 2004)] and $As^{5+}S_4$ tetrahedra [2.188 Å in billingsleyite (Bindi et al. 2010)]. The site distribution obtained is also in agreement with the bond valence sums calculated using the parameters given by Brese and O'Keeffe (1991), i.e., 1.04, 1.03, 0.92, 0.95, 0.90, 1.01, 1.04, and 0.90 valence unit (v.u.) for Ag1, Ag2, Ag3, Ag4, Ag5, Ag6, Ag7, and Ag8, respectively; 4.20 and 3.37 v.u. for $M1$ and $M2$ and 1.97, 2.19, 1.88, 2.07, 1.81, and 2.00 v.u. for S1, S2, S3, S4, S5, and S6, respectively.

Noteworthy, a network of non-interacting Ag cations is established for the mineral studied here. This behavior is different with respect to that usually reported for argyrodite-like compounds (Belin et al. 2001), which show a strong disorder in the sub-lattice of the moving cations at room temperature. As evident from the X-ray experiments carried out at low and high temperature, spryite maintains

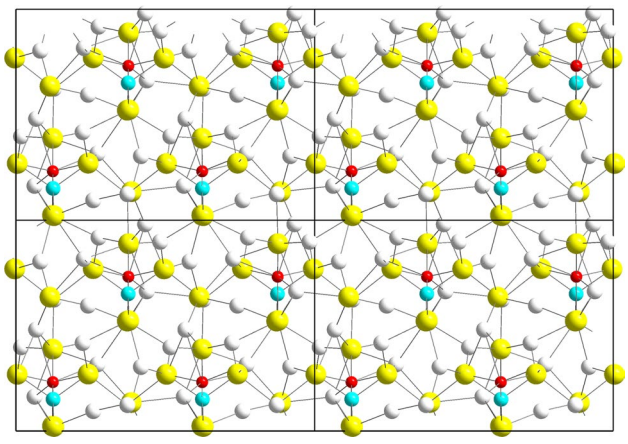

Fig. 4 Crystal structure of spryite as seen down [010]. *White*, *light blue*, *red,* and *yellow spheres* correspond to Ag, (Ge, As^{5+}), As^{3+}, and S, respectively

an orthorhombic structure over the temperature range (90–500 K) and it represents the first argyrodite-type compound which does not behave as a fast ionic conductor. Silver in argyrodite-type compounds is known to give such a high conductivity because of its preference for low coordination environments, which has been explained through band structure calculation by a *s/d* orbital mixing and polarization factors (Gaudin et al. 2001). Although we cannot be certain, it is very likely that the presence of As^{3+} in the argyrodite structure inhibits the typical ionic conductivity observed in these compounds. The presence of partially occupied $As^{3+}S_3$ pyramids could hinder the formation of the "quasi-liquid-like" structure of the mobile ions which usually are highly delocalized over the sites available to them. The free energy associated with the regular sites in spryite is likely higher than that of the interstitial sites, thus making the conduction mechanism highly unfavorable. Further studies would be needed to better characterize this compound and explore this hypothesis, but, unfortunately, the amount of available natural material precludes any additional investigation. However, spryite could be more common than thought and maybe additional material could be accessible from other sources. Indeed, a mineral with composition $Ag_{7.89}Cu_{0.03}Fe_{0.17}Zn_{0.02}Ge_{0.35}As_{0.59}S_{5.96}$ (nearly identical to spryite) was reported in the epithermal mineralization of the Capillitas deposit, Catamarca Province, Argentina (Putz et al. 2002; Putz 2005), associated with other Ge-bearing sulfides (putzite, $(Cu_{4.7}Ag_{3.3})_{\Sigma=8}GeS_6$, and catamarcaite, Cu_6GeWS_8) and proustite (Ag_3AsS_3) in silver-rich galena–sphalerite-rich ore from the Santa Rita Mina, La Argentina vein.

Acknowledgments The paper benefited by the official reviews made by Frantisek Laufek and Christopher Stanley. The research was supported by "progetto d'Ateneo 2013, University of Firenze" to L.B.

References

Belin R, Zerouale A, Pradel A, Ribes M (2001) Ion dynamics in the argyrodite compound Ag_7GeSe_5I: non-Arrhenius behavior and complete conductivity spectra. Solid State Ion 143:445–455

Bindi L, Evain M (2007) Gram-Charlier development of the atomic displacement factors into mineral structures: the case of samsonite, $Ag_4MnSb_2S_6$. Am Miner 92:886–891

Bindi L, Downs RT, Menchetti S (2010) The crystal structure of billingsleyite, $Ag_7(As, Sb)S_6$, a sulfosalt containing As^{5+}. Can Miner 48:155–162

Bindi L, Nestola F, Guastoni A, Zorzi F, Peruzzo L, Raber T (2012) Te-rich canfieldite, $Ag_8Sn(S, Te)_6$, from Lengenbach quarry, Binntal, Canton Valais, Switzerland: occurrence, description and crystal structure. Can Miner 50:111–118

Brese NE, O'Keeffe M (1991) Bond-valence parameters for solids. Acta Crystallogr B47:192–197

Chen HM, Maohua C, Adams S (2015) Stability and ionic mobility in argyrodite-related lithium-ion solid electrolytes. Phys Chem Chem Phys 17:16494–16506

Eulenberger G (1977) Die Kristallstrukture der Tieftemperaturmodifikation von Ag_8GeS_6. Monat Chem 108:901–913

Evain M, Gaudin E, Boucher F, Petříček V, Taule-lle F (1998) Structures and phase transitions of the A_7PSe_6 (A = Ag, Cu) argyrodite-type ionic conductors. I. Ag_7PSe_6. Acta Crystallogr B 54:376–383

Frank D, Gerke B, Eul M, Pöttgen R, Pfitzner A (2013) Synthesis and crystal structure determination of $Ag_9FeS_{4.1}Te_{1.9}$, the first example of an iron containing argyrodite. Chem Mater 25:2339–2345

Gaudin E, Boucher F, Evain M (2001) Some factors governing Ag^+ and Cu^+ low coordination in chalcogenide environments. J Solid State Chem 160:212–221

Gu X-P, Watanabe M, Hoshino K, Shibata Y (2003) New find of silver tellurosulphides from the Funan gold deposit, East Shandong, China. Eur J Miner 15:147–155

Gu X-P, Watanabe M, Xie X, Peng S, Nakamuta Y, Ohkawa M, Hoshino K, Ohsumi K, Shibata Y (2008) Chenguodaite ($Ag_9FeTe_2S_4$): a new tellurosulfide mineral from the gold district of East Shandong Peninsula, China. Chin Sci Bull 53:3567–3573

Kraus W, Nolze G (1996) PowderCell—a program for the representation and manipulation of crystal structures and calculation of the resulting X-ray powder patterns. J Appl Crystallogr 29:301–303

Kuhs WF, Nitsche R, Scheunemann K (1979) The argyrodites—a new family of tetrahedrally close-packed structures. Mater Res Bull 14:241–248

Oudin E, Picot P, Pillard F, Moëlo Y, Burke E, Zakrzewski A (1982) La benavidesite, $Pb_4(Mn, Fe)Sb_6S_{14}$, un nouveau mineral de la serie de la jamesonite. Bull Minér 105:166–169

Oxford Diffraction (2006) *CrysAlis* RED (Version 1.171.31.2) and ABSPACK in *CrysAlis* RED. Oxford Diffraction Ltd, Abingdon

Paar WH, Roberts AC, Berlepsch P, Armbruster T, Topa D, Zagler G (2004) Putzite, $(Cu_{4.7}Ag_{3.3})_8GeS_6$, a new mineral species from Capillitas, Catamarca, Argentina: description and crystal structure. Can Miner 42:1757–1769

Petříček V, Dušek M, Palatinus L (2006) JANA2006, a crystallographic computing system. Institute of Physics, Academy of Sciences of the Czech Republic, Prague

Putz H (2005) Mineralogy and genesis of epithermal ore deposits at Capillitas, Catamarca Province, NW Argentina. Ph.D. thesis, Salzburg Univ., Salzburg

Putz H, Paar WH, Sureda RJ, Roberts AC (2002) Germanium mineralization at Capillitas, Catamarca Province, Argentina. International Mineralogical Association, 18th General Meeting (Edinburgh), Abstract, 265

Rao RP, Adams S (2011) Studies of lithium argyrodite solid electrolytes for all-solid-state batteries. Phys Status Solidi A 208:1804–1807

Shannon RD (1976) Revised effective ionic radii and systematic studies of interatomic distances in halides and chalcogenides. Acta Crystallogr A 32:751–767

Wang N (1978) New data for Ag_8SnS_6 (canfieldite) and Ag_8GeS_6 (argyrodite). N Jahrb Miner Monat 1978:269–272

Weisbach A (1886) Argyrodit, ein neues Silbererz. N Jahrb Geol Paläont 2:67–71

Winkler C (1886) Germanium, Ge, a new nonmetallic element. Berichte der Deutschen Chem Gesell 19:210–211

Zucker UH, Schulz HH (1982) Statistical approaches for the treatment of anharmonic motion in crystals. II. Anharmonic thermal vibrations and effective atomic potentials in the fast ionic conductor lithium nitride (Li_3N). Acta Crystallogr A 38:568–576